Received: 18 September 2023 | Revised: 16 January 2024 | Accepted: 20 February 2024

DOI: 10.1002/nme.7469

RESEARCH ARTICLE

WILEY

Efficient stochastic modal decomposition methods for structural stochastic static and dynamic analyses

Zhibao Zheng[1] | **Michael Beer**[2,3,4] | **Udo Nackenhorst**[1]

[1]Institute of Mechanics and Computational Mechanics & International Research Training Group 2657, Leibniz Universität Hannover, Hannover, Germany

[2]Institute for Risk and Reliability, Leibniz Universität Hannover, Hannover, Germany

[3]Institute for Risk and Uncertainty and School of Engineering, University of Liverpool, Liverpool, UK

[4]International Joint Research Center for Resilient Infrastructure & International Joint Research Center for Engineering Reliability and Stochastic Mechanics, Tongji University, Shanghai, China

Correspondence
Zhibao Zheng, Leibniz Universität Hannover, Institute of Mechanics and Computational Mechanics, Appelstraße 9a, 30167, Hannover, Germany.
Email: zhibao.zheng@ibnm.uni-hannover.de

Funding information
Deutsche Forschungsgemeinschaft, Grant/Award Numbers: 527222589, 433082294; Alexander von Humboldt-Stiftung

Abstract

This article presents unified and efficient stochastic modal decomposition methods to solve stochastic structural static and dynamic problems. We extend the idea of deterministic modal decomposition method for structural dynamic analysis to stochastic cases. Standard/generalized stochastic eigenvalue equations are adopted to calculate the stochastic subspaces for stochastic static/dynamic problems and they are solved by an efficient reduced-order method. The stochastic solutions of both static and dynamic equations are approximated by stochastic bases of the stochastic subspaces. Original stochastic static/dynamic equations are then transformed into a set of single-degree-of-freedom (SDoF) stochastic static/dynamic equations, which are efficiently solved by the proposed non-intrusive methods. Specifically, a non-intrusive stochastic Newmark method is developed for the solution of SDoF stochastic dynamic equations, and the element-wise division of sample vectors is used to solve the SDoF stochastic static equations. All of these methods have low computational effort and are weakly sensitive to the stochastic dimension, thus the proposed methods avoid the curse of dimensionality successfully. Two numerical examples, including two- and three-dimensional spatial problems with low and high stochastic dimensions, are given to show the efficiency and accuracy of the proposed methods.

KEYWORDS

curse of dimensionality, stochastic eigenvalue problems, stochastic Newmark method, stochastic reduced-order equations, stochastic static and dynamic analyses

1 | INTRODUCTION

Predicting uncertainty propagation on the physical models has become an essential part in the analysis and design of practical engineering problems. The considerable influence of uncertainties on system behavior has led to the development of numerical methods for uncertainty analysis. In this article, we focus on developing efficient and unified numerical algorithms for linear stochastic static and dynamic analyses.

Many effective numerical methods have been developed for solving stochastic dynamic and static equations. The Monte Carlo simulation (MCS) and its extensions[1–3] have been widely used for the analyses. By repeatedly solving the

deterministic problem for each sample realization, they are executed in non-intrusive ways and can be readily applied to high-dimensional stochastic problems. However, they are usually computationally expensive since a large number of deterministic problems are solved to achieve high-accuracy stochastic solutions. Several more efficient non-intrusive methods, for example, adaptive sampling methods and response surface methods,[4–6] are also proposed for the purpose. As a kind of intrusive method, the Galerkin spectral stochastic finite element method and its extensions[7–9] have received a lot of attention for solving stochastic problems. In this method, the stochastic solution is decomposed into the summation of a series of products of polynomial chaos (PC) bases and deterministic time-independent/time-dependent functions. An augmented deterministic static/dynamic equation is then obtained by using the stochastic Galerkin projection. The size of the augmented equation is huge when dealing with large-scale and high-dimensional stochastic problems, thus this approach suffers from the curse of dimensionality. Several improvements are presented to reduce the computational effort of PC-based methods, for example, the Krylov-based iteration and the sparse PC approach.[10,11] Other methods are also explored to efficiently and accurately perform stochastic structural static and dynamic analyses, for example, the stochastic collocation method,[12] the PGD-based method,[13,14] the ANOVA method,[15] the direct probability integral method[16,17] and so forth.

We mention another kind of method, known as the modal decomposition-type method. Let us simply recall the idea of the modal decomposition method for solving deterministic structural dynamic equations.[18,19] In this method, a set of modes of the target system are calculated using a generalized eigenvalue equation and the time-dependent displacement response is solved by the linear superposition of each mode. It is natural and straightforward to extend the above idea of deterministic modal decomposition to the stochastic case, that is, stochastic eigenvalue equations are used to calculate a set of stochastic modes of the target stochastic system and the stochastic displacement is solved by the linear superposition of each stochastic mode. However, it is usually not a simple matter since efficient and accurate numerical algorithms are required to solve stochastic eigenvalue problems. Although a lot of methods can be used to solve stochastic eigenvalue equations, for example, the MCS,[20,21] the perturbation method,[22–24] the PC-based method,[25] the subspace iteration approach,[26–29] the stochastic collocation method,[30] the polynomial/spline dimensional decomposition methods,[31,32] the homotopy approach,[33] the low-rank approximation method[34,35] and so forth, only a few effort has been made to apply stochastic eigenvalue algorithms to modal decomposition-based stochastic dynamic analyses.

In References 36 and 37, the PC expansion is adopted to approximate stochastic eigenvalues, stochastic eigenvectors and stochastic responses, and stochastic Galerkin projection is used for their solutions. Similar to classical PC-based methods, this method still suffers from the curse of dimensionality, which is alleviated by a hybrid PC and MCS strategy in Reference 38. Also, another improvement is developed in Reference 26 by extending deterministic deflated and subspace inverse power methods to PC-based stochastic approaches, which can be applied to well solve the problems with repeated or closely spaced stochastic eigenvalues. The methods that combine PC-based stochastic finite element analyses with deterministic and stochastic reduced-order methods are developed in Reference 39, where deterministic/stochastic reduced bases are obtained by using deterministic/stochastic Krylov subspace techniques. In Reference 40, a high-order perturbation technique coupled with reduced modal subspaces is developed to solve stochastic dynamic systems, which exhibits better performance than the classical perturbation methods. The spline chaos expansion (SCE) and the spline dimensional decomposition (SDD) methods are proposed in Reference 41 for stochastic modal analyses. Similar to the PC expansion, both the two methods can be considered as Fourier-like expansions and the unknown expanded coefficients need to be calculated. An advantage of these two methods is that they can well capture nonlinear and nonsmooth stochastic solutions. Furthermore, SDD alleviates the curse of dimensionality encountered by SCE and classical PC-based methods.

In this article, we develop efficient and unified stochastic modal decomposition-based numerical schemes for solving stochastic static and dynamic problems. As discussed above, we construct stochastic subspaces for stochastic static/dynamic equations by solving standard/generalized stochastic eigenvalue equations. An efficient reduced-order method proposed in our prior work[42] is adopted for this purpose. In this method, stochastic eigenvectors are approximated by a set of products of random variables and deterministic vectors, where the deterministic vectors are calculated via a few number of deterministic eigenequations. A reduced-order stochastic eigenvalue problem constructed using the obtained deterministic vectors is then used to solve stochastic eigenvalues of the original problem and random variable coefficients corresponding to the deterministic vectors. Original stochastic static/dynamic equations are transformed into a set of SDoF stochastic static/dynamic equations by using the stochastic subspaces obtained by standard/generalized stochastic eigenequations. Following that, we develop a non-intrusive stochastic Newmark method to solve the SDoF stochastic dynamic equations and an element-wise division of sample vectors to solve the SDoF stochastic static equations. The proposed methods overcome the curse of dimensionality to a great extent since both the stochastic eigenvalue algorithm and

the approaches for solving SDoF stochastic static/dynamic equations are not sensitive to the stochastic dimension. Further, the final stochastic solutions of both stochastic static and dynamic problems can be represented as a sum of deterministic vectors with random variable coefficients, where the random variable coefficients are described by random samples. It is a kind of semiexplicit representation and provides a convenient pathway to perform uncertainty quantification.

The article is organized as follows: We extend the classical modal decomposition method to stochastic dynamic and static problems in Section 2, where an efficient reduced-order method is given to solve stochastic eigenvalue equations and generate stochastic subspaces for the stochastic modal decomposition method in Section 2.3. According to the obtained stochastic subspaces, stochastic static and dynamic equations are solved in Section 3. Algorithm implementations of the proposed methods are then elaborated in Section 4. Following that, two numerical examples are given to demonstrate the efficiency and accuracy of the proposed methods in Section 5, and conclusions follow in Section 6.

2 | STOCHASTIC MODAL DECOMPOSITION FOR STOCHASTIC STATIC AND DYNAMIC ANALYSIS

2.1 | Stochastic modal decomposition for stochastic dynamic analysis

Let $(\Theta, \Xi, \mathcal{P})$ be a suitable probability space, where Θ denotes the space of elementary events, Ξ is a σ-algebra defined on Θ and $\mathcal{P}$ is a probability measure. In this article, we consider a linear stochastic structural dynamic equation

$$\mathbf{M}(\theta)\ddot{\mathbf{u}}(t,\theta) + \mathbf{C}(\theta)\dot{\mathbf{u}}(t,\theta) + \mathbf{K}(\theta)\mathbf{u}(t,\theta) = \mathbf{F}(t,\theta) \tag{1}$$

defined on a deterministic domain $\mathcal{D} \subset \mathbb{R}^d$ with the physical dimension $d = 1, 2, 3$ and the boundary $\partial\mathcal{D}$, where $\mathbf{u}(t,\theta) \in \mathbb{R}^{n\times n_t}$ represents the unknown stochastic solution, n_t is the number of time steps, $\mathbf{u}(t_i,\theta) \in \mathbb{R}^n$ is the stochastic solution at the time step t_i, the symmetric and positive definite matrices $\mathbf{M}(\theta), \mathbf{C}(\theta), \mathbf{K}(\theta) \in \mathbb{R}^{n\times n}$, $\mathbf{F}(t,\theta) \in \mathbb{R}^{n\times n_t}$ are the stochastic mass matrix, the stochastic damping matrix, the stochastic stiffness matrix and the stochastic force vector, respectively, which are obtained by the classical finite element discretization, and the initial values are given by $\mathbf{u}(0,\theta) = \mathbf{u}_0(\theta) \in \mathbb{R}^n$ and $\dot{\mathbf{u}}(0,\theta) = \mathbf{u}_1(\theta) \in \mathbb{R}^n$. In this article, we only consider the Rayleigh damping, that is, $\mathbf{C}(\theta) = \varsigma_{\mathrm{M}}(\theta)\mathbf{M}(\theta) + \varsigma_{\mathrm{K}}(\theta)\mathbf{K}(\theta)$, where $\varsigma_{\mathrm{M}}(\theta)$ and $\varsigma_{\mathrm{K}}(\theta)$ are given (random) parameters. Hence, uncertainties of Equation (1) may be from stochastic material properties, stochastic forces, stochastic initial values and stochastic parameters in Rayleigh damping.

Inspired by the classical modal decomposition method for deterministic structural dynamic analysis,[18,43] we approximate the stochastic solution $\mathbf{u}(t,\theta)$ of Equation (1) as

$$\mathbf{u}(t,\theta) = \sum_{i=1}^{k} \boldsymbol{\varphi}_i(\theta) q_i(t,\theta) = \boldsymbol{\Phi}(\theta)\mathbf{q}(t,\theta), \tag{2}$$

where $\boldsymbol{\varphi}_i(\theta) \in \mathbb{R}^n$, $i = 1, \dots, k$ are a set of stochastic vectors that have determined in some way, $\boldsymbol{\Phi}(\theta) = \left[\boldsymbol{\varphi}_1(\theta), \dots, \boldsymbol{\varphi}_k(\theta)\right] \in \mathbb{R}^{n\times k}$ is a stochastic matrix (similar to the deterministic case, we name it as the stochastic subspace), $q_i(t,\theta) \in \mathbb{R}^{1\times n_t}$ are unknown time-dependent coefficients that need to be solved, $\mathbf{q}(t,\theta) = \left[q_1^{\mathrm{T}}(t,\theta), \dots, q_k^{\mathrm{T}}(t,\theta)\right]^{\mathrm{T}} \in \mathbb{R}^{k\times n_t}$ is the coefficient matrix, k is the dimension of the stochastic subspace $\boldsymbol{\Phi}(\theta)$. Substituting Equation (2) into Equation (1) we reformulate the stochastic dynamic equation as

$$\mathbf{M}(\theta)\boldsymbol{\Phi}(\theta)\ddot{\mathbf{q}}(t,\theta) + \mathbf{C}(\theta)\boldsymbol{\Phi}(\theta)\dot{\mathbf{q}}(t,\theta) + \mathbf{K}(\theta)\boldsymbol{\Phi}(\theta)\mathbf{q}(t,\theta) = \mathbf{F}(t,\theta), \tag{3}$$

which only has k unknown time-dependent variables $\{q_i(t,\theta)\}_{i=1}^k$ if the stochastic subspace $\boldsymbol{\Phi}(\theta)$ has been known, therefore we can solve it with less computational effort. To construct the stochastic subspace $\boldsymbol{\Phi}(\theta)$, the stochastic modes $\left\{\boldsymbol{\varphi}_i(\theta)\right\}_{i=1}^k$ are obtained by solving the following generalized stochastic eigenvalue equation

$$\mathbf{K}(\theta)\boldsymbol{\varphi}(\theta) = \lambda(\theta)\mathbf{M}(\theta)\boldsymbol{\varphi}(\theta), \tag{4}$$

whose solution algorithm will be discussed in detail in Section 2.3. In this way, the stochastic matrix $\boldsymbol{\Phi}(\theta)$ meets $\boldsymbol{\Phi}^{\mathrm{T}}(\theta)\boldsymbol{\Phi}(\theta) = \mathbf{I}_k \in \mathbb{R}^{k\times k}$ almost everywhere (a.e.), where $\mathbf{I}_k$ represents the identity matrix. Taking advantage of this and

recalling Equation (2) we have $q_i(t,\theta) = \boldsymbol{\varphi}_i^{\mathrm{T}}(\theta)\mathbf{u}(t,\theta)$, which results in $q_i(t,\theta)$ still depending on the random input θ. However, as presented later, $q_i(t,\theta)$ can be solved cheaply via a one-dimensional stochastic problem benefiting from the orthogonality of $\boldsymbol{\Phi}(\theta)$. Furthermore, the stochastic modes $\boldsymbol{\varphi}_i(\theta)$ and $\boldsymbol{\varphi}_j(\theta)$ corresponding to different stochastic eigenvalues $\lambda_i(\theta)$ and $\lambda_j(\theta)$ (i.e., $i \neq j$) meet the orthogonal conditions

$$\boldsymbol{\varphi}_i^{\mathrm{T}}(\theta)\mathbf{M}(\theta)\boldsymbol{\varphi}_j(\theta) = 0, \quad \boldsymbol{\varphi}_i^{\mathrm{T}}(\theta)\mathbf{K}(\theta)\boldsymbol{\varphi}_j(\theta) = 0 \qquad \text{a.e.}, \tag{5}$$

whose proof is found in the Appendix. In other words, although Equation (5) is dependent of the random input, the above orthogonal conditions hold over the spatial domain for each realization of $\theta \in \Theta$, which thus allows the construction of decoupled stochastic problems to solve the coefficients $\{q_i(t,\theta)\}_{i=1}^k$.

To solve unknown stochastic coefficients $\{q_i(t,\theta)\}_{i=1}^k$ in Equation (3), multiplying Equation (3) by $\boldsymbol{\Phi}^{\mathrm{T}}(\theta)$ from left and taking advantage of the orthogonality in Equation (5) we have

$$\mathbf{m}(\theta)\ddot{\mathbf{q}}(t,\theta) + \mathbf{c}(\theta)\dot{\mathbf{q}}(t,\theta) + \mathbf{k}(\theta)\mathbf{q}(t,\theta) = \mathbf{f}(t,\theta) \tag{6}$$

with the initial values $\mathbf{q}_0(\theta) = \mathbf{q}(0,\theta) = \boldsymbol{\Phi}^{\mathrm{T}}(\theta)\mathbf{u}_0(\theta) \in \mathbb{R}^k$ and $\mathbf{q}_1(\theta) = \dot{\mathbf{q}}(0,\theta) = \boldsymbol{\Phi}^{\mathrm{T}}(\theta)\mathbf{u}_1(\theta) \in \mathbb{R}^k$, where the diagonal stochastic matrices $\mathbf{m}(\theta)$, $\mathbf{k}(\theta)$, $\mathbf{c}(\theta) \in \mathbb{R}^{k\times k}$ and the stochastic vector $\mathbf{f}(t,\theta) \in \mathbb{R}^{k\times n_t}$ are given by

$$\begin{aligned}
\mathbf{m}(\theta) &= \boldsymbol{\Phi}^{\mathrm{T}}(\theta)\mathbf{M}(\theta)\boldsymbol{\Phi}(\theta) = \begin{bmatrix} m_1(\theta) & & 0 \\ & \ddots & \\ 0 & & m_k(\theta) \end{bmatrix}, \\
\mathbf{k}(\theta) &= \boldsymbol{\Phi}^{\mathrm{T}}(\theta)\mathbf{K}(\theta)\boldsymbol{\Phi}(\theta) = \begin{bmatrix} k_1(\theta) & & 0 \\ & \ddots & \\ 0 & & k_k(\theta) \end{bmatrix}, \\
\mathbf{c}(\theta) &= \boldsymbol{\Phi}^{\mathrm{T}}(\theta)\mathbf{C}(\theta)\boldsymbol{\Phi}(\theta) = \varsigma_{\mathrm{M}}(\theta)\mathbf{m}(\theta) + \varsigma_{\mathrm{K}}(\theta)\mathbf{k}(\theta), \\
\mathbf{f}(t,\theta) &= \boldsymbol{\Phi}^{\mathrm{T}}(\theta)\mathbf{F}(t,\theta) = \left[f_1(t,\theta), \ \dots \ , f_k(t,\theta)\right]^{\mathrm{T}}.
\end{aligned} \tag{7}$$

Since the matrices $\mathbf{m}(\theta)$, $\mathbf{k}(\theta)$ and $\mathbf{c}(\theta)$ are diagonal, Equation (6) can be decoupled into k SDoF stochastic dynamic equations

$$m_i(\theta)\ddot{q}_i(t,\theta) + c_i(\theta)\dot{q}_i(t,\theta) + k_i(\theta)q_i(t,\theta) = f_i(t,\theta) \tag{8}$$

for $i = 1, \ \dots \ , k$, which is further simplified as

$$\ddot{q}_i(t,\theta) + \varpi_i(t,\theta)\dot{q}_i(t,\theta) + \lambda_i(\theta)q_i(t,\theta) = h_i(t,\theta) \tag{9}$$

by a normalizing procedure

$$\begin{aligned}
\frac{k_i(\theta)}{m_i(\theta)} &= \frac{\boldsymbol{\varphi}_i^{\mathrm{T}}(\theta)\mathbf{K}(\theta)\boldsymbol{\varphi}_i(\theta)}{\boldsymbol{\varphi}_i^{\mathrm{T}}(\theta)\mathbf{M}(\theta)\boldsymbol{\varphi}_i(\theta)} = \lambda_i(\theta), \\
\frac{c_i(\theta)}{m_i(\theta)} &= \frac{\boldsymbol{\varphi}_i^{\mathrm{T}}(\theta)\mathbf{C}(\theta)\boldsymbol{\varphi}_i(\theta)}{\boldsymbol{\varphi}_i^{\mathrm{T}}(\theta)\mathbf{M}(\theta)\boldsymbol{\varphi}_i(\theta)} = \varsigma_{\mathrm{M}}(\theta) + \varsigma_{\mathrm{K}}(\theta)\lambda_i(\theta) := \varpi_i(\theta), \\
\frac{f_i(t,\theta)}{m_i(\theta)} &= \frac{\boldsymbol{\varphi}_i^{\mathrm{T}}(\theta)\mathbf{F}(t,\theta)}{\boldsymbol{\varphi}_i^{\mathrm{T}}(\theta)\mathbf{M}(\theta)\boldsymbol{\varphi}_i(\theta)} := h_i(t,\theta).
\end{aligned} \tag{10}$$

In this way, we transform the original stochastic dynamic equation into k SDoF stochastic dynamic equations (9) (i.e., one-dimensional second order stochastic ordinary differential equations), which can be solved by existing ODE solvers.[44] In this article, we will efficiently solve Equation (9) by using a stochastic Newmark method in Section 3.2. Further, Equation (1) degenerates into a deterministic dynamical equation for each realization of $\theta \in \Theta$. In this way, Equation (2)

to Equation (10) are the same as the procedure of the classical modal decomposition method. Therefore, the existence and well-posedness of the above stochastic solution can be inherited from the classical modal decomposition method in a probabilistic sense.

2.2 | Stochastic modal decomposition for stochastic static analysis

The above procedure for solving stochastic dynamic equations can be readily extended to stochastic static problems. Typically, it is unnecessary to solve deterministic static problems by modal decomposition-type methods due to the well-established deterministic solvers. However, efficient stochastic solvers for stochastic static problems are still worth studying. The stochastic modal decomposition method in this article provides a new approach for this purpose. Specifically, we consider the following linear stochastic finite element equation

$$\mathbf{K}(\theta)\mathbf{u}(\theta) = \mathbf{F}(\theta) \tag{11}$$

defined on a deterministic domain $\mathcal{D} \subset \mathbb{R}^d$ with the boundary $\partial\mathcal{D}$, where $\mathbf{u}(\theta) \in \mathbb{R}^n$ is the unknown stochastic solution, the symmetric and positive definite stochastic stiffness matrix $\mathbf{K}(\theta) \in \mathbb{R}^{n\times n}$ is the same as that given in Equation (1) and $\mathbf{F}(\theta) \in \mathbb{R}^n$ is a time-independent stochastic force vector. Similar to Equation (2), we approximate the stochastic solution $\mathbf{u}(\theta)$ of Equation (11) by

$$\mathbf{u}(\theta) = \sum_{i=1}^{k} \boldsymbol{\varphi}_i(\theta) q_i(\theta) = \boldsymbol{\Phi}(\theta)\mathbf{q}(\theta), \tag{12}$$

where the stochastic vectors $\boldsymbol{\varphi}_i(\theta) \in \mathbb{R}^n$, $i = 1, \dots, k$ and the stochastic subspace $\boldsymbol{\Phi}(\theta) \in \mathbb{R}^{n\times k}$ has the same form given in Equation (2) and $\mathbf{q}(\theta) = \left[q_1(\theta), \dots, q_k(\theta)\right]^{\mathrm{T}} \in \mathbb{R}^k$ are unknown time-independent stochastic coefficients that need to be solved. To calculate the stochastic subspace $\boldsymbol{\Phi}(\theta)$, only a standard stochastic eigenvalue equation is required to solve in this case

$$\mathbf{K}(\theta)\boldsymbol{\varphi}(\theta) = \lambda(\theta)\boldsymbol{\varphi}(\theta), \tag{13}$$

whose solution algorithm is the same as that for Equation (4) and will be discussed in Section 2.3. Substituting Equation (12) into Equation (11) and multiplying it by $\boldsymbol{\Phi}^{\mathrm{T}}(\theta)$ from left we have

$$\mathbf{k}(\theta)\mathbf{q}(\theta) = \mathbf{f}(\theta), \tag{14}$$

where the diagonal stochastic matrix $\mathbf{k}(\theta) \in \mathbb{R}^{k\times k}$ and the stochastic vector $\mathbf{f}(\theta) \in \mathbb{R}^k$ are given in similar ways as in Equation (7)

$$\mathbf{k}(\theta) = \boldsymbol{\Phi}^{\mathrm{T}}(\theta)\mathbf{K}(\theta)\boldsymbol{\Phi}(\theta) = \begin{bmatrix} \lambda_1(\theta) & & 0 \\ & \ddots & \\ 0 & & \lambda_k(\theta) \end{bmatrix}, \quad \mathbf{f}(\theta) = \boldsymbol{\Phi}^{\mathrm{T}}(\theta)\mathbf{F}(\theta) = \begin{bmatrix} f_1(\theta) \\ \vdots \\ f_k(\theta) \end{bmatrix}. \tag{15}$$

Thus, Equation (14) are also decoupled into k SDoF stochastic static equations

$$\lambda_i(\theta) q_i(\theta) = f_i(\theta) \tag{16}$$

for $i = 1, \dots, k$, which are one-dimensional stochastic algebraic equations and will be solved by a nonintrusive method in Section 3.3.

2.3 | An iterative algorithm for solving stochastic eigenvalue equations

As discussed above, the key issues of both the stochastic static and dynamic problems are to solve standard/generalized stochastic eigenvalue equations. In this section, we give an effective solution algorithm for this purpose. Here we only

consider the generalized stochastic eigenvalue problem Equation (4), which degenerates to the standard stochastic eigenvalue problem Equation (13) by simply letting $\mathbf{M}(\theta)$ be the identity matrix $\mathbf{I}_n$. The authors have developed an efficient reduced-order method to solve stochastic eigenvalue problems in Reference 42. In this section, we recall the idea and apply it to solve the stochastic static and dynamic equations. To solve Equation (4), we approximate the ith stochastic eigenvector $\boldsymbol{\varphi}_i(\theta)$ by

$$\boldsymbol{\varphi}_i(\theta) = \sum_{j=1}^{r} \eta_{ij}(\theta)\mathbf{d}_j = \mathbf{D}\boldsymbol{\eta}_i(\theta) \tag{17}$$

for $i = 1, 2, \ldots$, where $\mathbf{d}_j \in \mathbb{R}^n$ are deterministic vectors, $\mathbf{D} = [\mathbf{d}_1, \ldots, \mathbf{d}_r] \in \mathbb{R}^{n\times r}$ is a deterministic matrix, $\eta_{ij}(\theta) \in \mathbb{R}$ are scalar random variables, $\boldsymbol{\eta}_i(\theta) = [\eta_{i1}(\theta), \ldots, \eta_{ir}(\theta)]^{\mathrm{T}} \in \mathbb{R}^r$ represents the random variable vector, r is the number of approximate terms, which requires to meet $r \geq k$ in order to provide a high-accuracy approximation. In practical implementations, we simply let the number $r = k$.

Both the random variables $\left\{\eta_{ij}(\theta)\right\}_{j=1}^{r}$ and the deterministic vectors $\left\{\mathbf{d}_j\right\}_{j=1}^{r}$ are not known a priori. According to Reference 42, the vectors $\left\{\mathbf{d}_j\right\}_{j=1}^{r}$ are solved by the following alternating iteration

$$\mathbb{E}\left\{\lambda_j(\theta)\mathbf{K}(\theta)\right\}\mathbf{d}_j = \mathbb{E}\left\{\lambda_j^2(\theta)\mathbf{M}(\theta)\right\}\mathbf{d}_j, \tag{18a}$$

$$\left[\mathbf{d}_j^{\mathrm{T}}\mathbf{M}(\theta)\mathbf{d}_j\right]\lambda_j(\theta) = \mathbf{d}_j^{\mathrm{T}}\mathbf{K}(\theta)\mathbf{d}_j, \tag{18b}$$

where $\mathbb{E}\{\cdot\}$ is the expectation operator. Equation (18a) is obtained taking advantage of the stochastic Galerkin method[7,8] for a known random variable $\lambda_j(\theta)$ (or given an initial value). The vector $\mathbf{d}_j$ can be solved efficiently by use of existing deterministic eigenvalue solvers.[45] For the modal decomposition analysis, we only need to solve the first few stochastic eigenvectors and the inverse power iteration is adopted in this article. In numerical implementations, we make the vector $\mathbf{d}_j$ orthogonal to the obtained vectors $\{\mathbf{d}_i\}_{i=1}^{j-1}$, which achieves by Gram-Schmidt orthogonalization. With the known $\mathbf{d}_j$, Equation (18b) is obtained by the classical Galerkin procedure. Note that it is a one-dimensional stochastic algebraic equation that can be solved efficiently in a non-intrusive sampling way using n_s random sample realizations. Similarly, the deterministic matrix $\mathbb{E}\left\{\lambda_j(\theta)\mathbf{K}(\theta)\right\} = 1/n_s\sum_{i=1}^{n_s}\lambda_j\left(\theta^{(i)}\right)\mathbf{K}\left(\theta^{(i)}\right) \in \mathbb{R}^{n\times n}$ can be estimated cheaply using n_s random sample realizations. We can obtain the couple $\left\{\lambda_j(\theta), \mathbf{d}_j\right\}$ by repeatedly solving Equations (18a) and (18b) until convergence. The random variable vector $\boldsymbol{\eta}_i(\theta)$ is then solved based on the known matrix $\mathbf{D} = [\mathbf{d}_1, \ldots, \mathbf{d}_r]$. Substituting Equation (17) into Equation (4) and multiplying Equation (4) by $\mathbf{D}^{\mathrm{T}}$ from left we have

$$\left[\mathbf{D}^{\mathrm{T}}\mathbf{K}(\theta)\mathbf{D}\right]\boldsymbol{\eta}_i(\theta) = \lambda_i(\theta)\left[\mathbf{D}^{\mathrm{T}}\mathbf{M}(\theta)\mathbf{D}\right]\boldsymbol{\eta}_i(\theta), \tag{19}$$

which is a reduced-order stochastic eigenvalue equation of size r. We adopt the sampling method to solve Equation (19), which has low computational effort thanking to its small size. In practice, we only need to solve the first few stochastic eigenvectors $\left\{\boldsymbol{\eta}_i(\theta)\right\}_{i=1}^{r}$ of the reduced-order stochastic eigenproblem (19) to approximate the stochastic eigenvectors $\left\{\boldsymbol{\varphi}_i(\theta)\right\}_{i=1}^{k}$ of the original stochastic eigenproblem (4). It is noted that Equations (18a), (18b), and (19) are weakly dependent on the stochastic dimension, thus the proposed method can be applied to very high-dimensional stochastic problems. Details of numerical implementations of the above iterative process can be found in Reference 42.

3 | SOLUTION ALGORITHMS BASED ON STOCHASTIC MODAL DECOMPOSITION

3.1 | Stochastic modal decomposition-based stochastic static and dynamic analysis

Recalling the SDoF stochastic dynamic and static problems Equations (9) and (16), we can calculate the stochastic eigenvalues $\{\lambda_i(\theta)\}_{i=1}^{k}$ via solving the reduced-order stochastic eigenproblem (19) and no additional computational effort is required. According to Equation (17), the right-side terms of Equations (9) and (16) are calculated by

$$h_i(t,\theta) = \frac{\boldsymbol{\eta}_i^{\mathrm{T}}(\theta)\mathbf{D}^{\mathrm{T}}\mathbf{F}(t,\theta)}{\boldsymbol{\eta}_i^{\mathrm{T}}(\theta)\mathbf{D}^{\mathrm{T}}\mathbf{M}(\theta)\mathbf{D}\boldsymbol{\eta}_i(\theta)}, \tag{20a}$$

$$f_i(\theta) = \boldsymbol{\eta}_i^{\mathrm{T}}(\theta)\mathbf{D}^{\mathrm{T}}\mathbf{F}(\theta). \tag{20b}$$

In this way, we reformulate the SDoF stochastic equations (9) and (16) based on the proposed stochastic eigenvalue algorithm. There is no reformulation to the left sides and only slight modifications to the right-side terms are required.

3.2 | Solution algorithm for SDoF stochastic dynamic equations

In this section, we extend the deterministic Newmark method to solve the SDoF stochastic dynamic equation (9). According to the classical Newmark method,[18,46] the stochastic solution $q_i(t+\Delta t,\theta)$ at the time $t+\Delta t$ is solved based on the stochastic solution $q_i(t,\theta)$ at the time t and the time increment Δt, which corresponds to

$$s_i(\theta)q_i(t+\Delta t,\theta) = z_i(t+\Delta t,\theta), \tag{21}$$

where the random variables $s_i(\theta) = \alpha_1 + \alpha_2\varpi_i(\theta) + \lambda_i(\theta)$ and $z_i(t+\Delta t,\theta) = h_i(t+\Delta t,\theta) + \alpha_{9,k}(\theta)q_i(t,\theta) + \alpha_{10,k}(\theta)\dot{q}_i(t,\theta) + \alpha_{11,k}(\theta)\ddot{q}_i(t,\theta)$, the parameters $\alpha_1 = \frac{1}{\beta\Delta t^2}$, $\alpha_2 = \frac{\gamma}{\beta\Delta t}$, $\alpha_3 = \frac{1}{\beta\Delta t}$, $\alpha_4 = \frac{1}{2\beta} - 1$, $\alpha_5 = \frac{\gamma}{\beta} - 1$, $\alpha_6 = \frac{\Delta t}{2}\left(\frac{\gamma}{\beta} - 2\right)$, $\alpha_7 = \Delta t(1-\gamma)$, $\alpha_8 = \gamma\Delta t$ are inherited from the classical Newmark method. They are fixed for the given time discretization and the chosen parameters γ, β. Also, the parameters $\alpha_{9,i}(\theta)$, $\alpha_{10,i}(\theta)$ and $\alpha_{11,i}(\theta)$ are random variables given by $\alpha_{9,i}(\theta) = \alpha_1 + \alpha_2\varpi_i(\theta)$, $\alpha_{10,i}(\theta) = \alpha_3 + \alpha_5\varpi_i(\theta)$ and $\alpha_{11,i}(\theta) = \alpha_4 + \alpha_6\varpi_i(\theta)$. We solve Equation (21) using a nonintrusive approach

$$\widehat{q}_i(t+\Delta t,\widehat{\boldsymbol{\theta}}) = \widehat{z}_i(t+\Delta t,\widehat{\boldsymbol{\theta}}) \oslash \widehat{s}_i(\widehat{\boldsymbol{\theta}}) \in \mathbb{R}^{n_s}, \tag{22}$$

where $\oslash$ is the Hadamard division operator representing the element-wise division of two vectors. It is numerically stable since $s_i(\theta) > 0$ holds for all $\theta \in \Theta$. The random variable $s_i(\theta)$ is fixed for different time t, but the random variable $z_i(t+\Delta t,\theta)$ needs to be updated for each time step. To solve the stochastic solution of the next time step, the first and second derivatives $\ddot{q}_i(t+\Delta t,\theta)$ and $\dot{q}_i(t+\Delta t,\theta)$ are calculated based on $\widehat{q}_i(t+\Delta t,\widehat{\boldsymbol{\theta}})$ in a similar way to the classical Newmark method.

3.3 | Solution algorithm for SDoF stochastic static equations

In this section, we focus on solving the SDoF stochastic static equation (16). Similar to Equation (22), it is easily solved by using the proposed non-intrusive approach

$$\widehat{q}_i(\widehat{\boldsymbol{\theta}}) = \widehat{f}_i(\widehat{\boldsymbol{\theta}}) \oslash \widehat{\lambda}_i(\widehat{\boldsymbol{\theta}}) \in \mathbb{R}^{n_s}, \tag{23}$$

where the the random sample vectors are given by $\widehat{f}_i(\widehat{\boldsymbol{\theta}}) \in \mathbb{R}^{n_s}$ and $\widehat{\lambda}_i(\widehat{\boldsymbol{\theta}}) \in \mathbb{R}^{n_s}$. We can thus recover the stochastic solution $\mathbf{u}(\theta)$ in Equation (12) as

$$\mathbf{u}(\theta) = \mathbf{D}\boldsymbol{\Pi}(\theta)\mathbf{q}(\theta) = \mathbf{D}\boldsymbol{\Psi}(\theta), \tag{24}$$

where $\boldsymbol{\Pi}(\theta) = \left[\boldsymbol{\eta}_1(\theta), \ldots, \boldsymbol{\eta}_k(\theta)\right] \in \mathbb{R}^{r\times k}$ is a random variable matrix and a new random variable vector is given by $\boldsymbol{\Psi}(\theta) = \boldsymbol{\Pi}(\theta)\mathbf{q}(\theta) \in \mathbb{R}^r$. In this way, we decouple the stochastic solution $\mathbf{u}(\theta)$ into stochastic and deterministic spaces and all the randomness is embedded into the random variable vector $\boldsymbol{\Psi}(\theta)$, which is more convenient for uncertainty quantification. Also, we can use a similar way to recover the stochastic solution of the stochastic dynamic equation

$$\mathbf{u}(t,\theta) = \mathbf{D}\boldsymbol{\Pi}(\theta)\mathbf{q}(t,\theta) = \mathbf{D}\boldsymbol{\Psi}(t,\theta), \tag{25}$$

where $\boldsymbol{\Psi}(t,\theta) = \boldsymbol{\Pi}(\theta)\mathbf{q}(t,\theta)$ is a time-dependent random variable vector.

Remark 1. Inspired by the decoupled representation Equations (24) and (25), we can also transform the stochastic dynamic equation (1) into a reduced-order stochastic dynamic equation

$$\left[\mathbf{D}^{\mathrm{T}}\mathbf{M}(\theta)\mathbf{D}\right]\ddot{\mathbf{q}}(t,\theta)+\left[\mathbf{D}^{\mathrm{T}}\mathbf{C}(\theta)\mathbf{D}\right]\dot{\mathbf{q}}(t,\theta)+\left[\mathbf{D}^{\mathrm{T}}\mathbf{K}(\theta)\mathbf{D}\right]\mathbf{q}(t,\theta)=\mathbf{D}^{\mathrm{T}}\mathbf{F}(t,\theta) \tag{26}$$

by introducing $\mathbf{u}(t,\theta)=\mathbf{D}\,\mathbf{q}(t,\theta)$, and transform the stochastic static equation (11) into a reduced-order stochastic static equation

$$\left[\mathbf{D}^{\mathrm{T}}\mathbf{K}(\theta)\mathbf{D}\right]\mathbf{q}(\theta)=\mathbf{D}^{\mathrm{T}}\mathbf{F}(\theta) \tag{27}$$

by introducing $\mathbf{u}(\theta)=\mathbf{D}\,\mathbf{q}(\theta)$, where the matrix $\mathbf{D}$ is given in Equation (17), $\mathbf{q}(\theta)$ and $\mathbf{q}(t,\theta)$ are the unknown stochastic coefficients that need to be solved. We can solve both Equations (26) and (27) by sample-based methods, that is, solving them for each sample realization $\theta^{(i)}$, $i=1,\ \dots\ ,n_s$, which is still cheap since the sizes of the reduced-order equations are small in most cases. We remark that similar reduced-order equations have been studied in References 47 and 48, but in which the deterministic matrix $\mathbf{D}$ is obtained by other iterative algorithms and they are considered as a kind of deterministic reduced-order method. As a comparison, the proposed methods in this article are kinds of stochastic reduced-order methods. In this article, by taking advantage of the orthogonality, only SDoF stochastic dynamic/static equations require to be solved, while one has to solve k degrees-of-freedom systems of stochastic linear dynamic/static equations for Equations (26) and (27), and the size k has a significant influence on the computational effort.

4 | ALGORITHM IMPLEMENTATION

In this section, we give the details of algorithm implementations of the proposed methods. The method for solving stochastic dynamic equations is summarized in Algorithm 1. To generate the stochastic subspace, stochastic eigenvalues and stochastic eigenvectors are solved in step 1 via the stochastic eigenvalue Algorithm 3. After that, the SDoF stochastic dynamic equation (9) is solved by two loops, where the outer loop that is from step 2 to step 10 is used to solve the stochastic solution $q_i(t,\theta)$ corresponding to the ith stochastic mode, and the inner loop that is from step 3 to step 9 is used to solve the stochastic solution $q_i\left(t_j,\theta\right)$ of the time step t_j. For the inner loop, the random sample vectors $\widehat{s}_i(\widehat{\boldsymbol{\theta}})\in\mathbb{R}^{n_s}$ is precomputed once, but $\widehat{z}_i\left(t_j,\widehat{\boldsymbol{\theta}}\right)\in\mathbb{R}^{n_s}$ is calculated for each time step based on the results of previous time step. Also, the first and second derivatives are required to be calculated in step 8. After the two loops, the stochastic solution $\mathbf{u}(t,\theta)$ is reconstructed in step 11.

Further, the proposed method for solving stochastic static equations is listed in Algorithm 2. The stochastic eigenvalue Algorithm 3 is still used in step 1 to generate the stochastic subspace. Only one loop that is from step 2 to step 5 is involved

Algorithm 1. Stochastic modal decomposition for solving stochastic dynamic equations

1: Solve stochastic eigenvalues and eigenvectors via the stochastic eigenvalue Algorithm 3
2: **for** $i=1,\dots,k$ **do**
3: Calculate $\widehat{s}_i\left(\widehat{\boldsymbol{\theta}}\right)\in\mathbb{R}^{n_s}$
4: **for** $j=1,\dots,n_t$ **do**
5: Calculate the ith right-side term $\widehat{h}_i\left(t_j,\widehat{\boldsymbol{\theta}}\right)\in\mathbb{R}^{n_s}$ by Equation (20a)
6: Calculate $\widehat{z}_i\left(t_j,\widehat{\boldsymbol{\theta}}\right)\in\mathbb{R}^{n_s}$
7: Solve the stochastic solution $\widehat{q}_i\left(t_j,\widehat{\boldsymbol{\theta}}\right)\in\mathbb{R}^{n_s}$ at the time step t_j by Equation (22)
8: Calculate the second and first derivatives $\ddot{\widehat{q}}_i\left(t_j,\widehat{\boldsymbol{\theta}}\right),\dot{\widehat{q}}_i\left(t_j,\widehat{\boldsymbol{\theta}}\right)\in\mathbb{R}^{n_s}$ at the time step t_j
9: **end for**
10: **end for**
11: Recover the stochastic solution $\mathbf{u}\,(t,\theta)$ using Equation (25)

Algorithm 2. Stochastic modal decomposition for solving stochastic static equations

1: Solve stochastic eigenvalues and eigenvectors via the stochastic eigenvalue Algorithm 3
2: **for** $i = 1, \dots, k$ **do**
3: Calculate the ith right-side term $\widehat{f}_i\left(\widehat{\theta}\right) \in \mathbb{R}^{n_s}$ by Equation (20b)
4: Solve the stochastic solution $\widehat{q}_i\left(\widehat{\theta}\right) \in \mathbb{R}^{n_s}$ by Equation (23)
5: **end for**
6: Recover the stochastic solution $\mathbf{u}(\theta)$ using Equation (24)

Algorithm 3. Iterative algorithm for solving stochastic eigenvalue equations

1: Assemble stochastic matrices $\mathbf{K}(\theta)$ and $\mathbf{M}(\theta)$ ($= \mathbf{I}_n$ if *Stochastic static problems*)
2: **while** $\epsilon_{\text{ev},j} > \epsilon_{\text{ev}}$ **do**
3: Initialize the random sample vector $\widehat{\lambda}_j^{(0)}\left(\widehat{\theta}\right) \in \mathbb{R}^{n_s}$
4: **while** $\epsilon_{\mathbf{d},m} > \epsilon_{\mathbf{d}}$ **do**
5: Solve the deterministic vector $\mathbf{d}_j^{(m)}$ by the inverse power iteration
6: Solve the random variable $\widehat{\lambda}_j^{(m)}\left(\widehat{\theta}\right) \in \mathbb{R}^{n_s}$ by Equation (18b)
7: Calculate the iterative error $\epsilon_{\mathbf{d},m}$, $m \leftarrow m + 1$
8: **end while**
9: Update the matrix $\mathbf{D} = \left[\mathbf{D}, \mathbf{d}_j\right] \in \mathbb{R}^{n \times j}$
10: Calculate the iterative error $\epsilon_{\text{ev},j}$, $j \leftarrow j + 1$
11: **end while**
12: Calculate reduced-order eigenpairs $\left\{\lambda_i(\theta), \boldsymbol{\eta}_i(\theta)\right\}_{i=1}^{k}$ by Equation (19)
13: Calculate the ith original stochastic eigenvector $\boldsymbol{\varphi}_i(\theta) = \mathbf{D}\boldsymbol{\eta}_i(\theta)$ via Equation (17)

to solve the stochastic solution $q_i(\theta)$ corresponding to the ith stochastic mode. Compared to the stochastic dynamic case, both the random sample vector $\widehat{\lambda}_i(\widehat{\boldsymbol{\theta}}) \in \mathbb{R}^{n_s}$ and $\widehat{f}_i(\widehat{\boldsymbol{\theta}}) \in \mathbb{R}^{n_s}$ are calculated once. Thus the computational effort for solving the stochastic solution $\widehat{q}_i(\widehat{\boldsymbol{\theta}}) \in \mathbb{R}^{n_s}$ in step 4 is very low. Finally the stochastic solution $\mathbf{u}(t, \theta)$ is reconstructed in step 6. Furthermore, we highlight both Algorithms 1 and 2 have good parallelizability since Equations (9) and (16) can be solved in parallel for each stochastic mode $i = 1, \dots, k$. Their solution processes are completely independent.

Both Algorithms 1 and 2 require generating the stochastic subspace using the stochastic eigenvalue algorithm, which has been studied in detail in Reference 42 and only a simplified version of which is adopted in this article. To clearly implement the proposed methods, we review its implementation in Algorithm 3. The stochastic stiffness matrices are assembled in step 1. It is noted that only a standard stochastic eigenvalue equation is solved for stochastic static problems and it is achieved by letting the stochastic mass matrix $\mathbf{M}(\theta) = \mathbf{I}_n$. There are two loops involved, where the outer loop that is from step 2 to step 11 is used to solve all couples $\{\lambda_i(\theta), \mathbf{d}_i\}_{i=1}^{j}$ and the inner loop that is from step 4 to step 8 is used to calculate each couple $\{\lambda_i(\theta), \mathbf{d}_i\}$. The stopping criteria of the inner and outer loops are given by $\epsilon_{\mathbf{d},m} = \left\|\mathbf{d}_j^{(m)} - \mathbf{d}_j^{(m-1)}\right\|$ and $\epsilon_{\text{ev},j} = \mathbb{E}\left\{\lambda_1^2(\theta)\right\} / \sum_{i=1}^{j} \mathbb{E}\left\{\lambda_i^2(\theta)\right\}$, respectively.

5 | NUMERICAL EXAMPLES

In this section, we test the proposed stochastic modal decomposition (SMD) methods with the aid of two numerical examples. For both examples, the stopping criterion $\epsilon_{\mathbf{d},m}$ of the inner loop of Algorithm 3 is set as 1×10^{-3}, and $\epsilon_{\text{ev},j}$ of the outer loop of Algorithm 3 is set as 1×10^{-6}. The parameters in Rayleigh damping are simply set as $\varsigma_{\text{M}}(\theta) = 10$ rad/s and $\varsigma_{\text{K}}(\theta) = 0$ s/rad, which is just a simple setting and the values can be changed to fit more realistic situations. Parameters of the stochastic Newmark method are $\beta = 0.25$ and $\gamma = 0.5$. Reference solutions are obtained by directly solving Equation (1) in the time domain using the standard MCS-based stochastic Newmark method. It has been verified that

1×10^4 MCS can reach converged reference solutions. Furthermore, to eliminate the influence caused by sampling processes, the same 1×10^4 random sample realizations are used to the proposed SMD methods too. All examples are performed on a desktop computer (sixteen cores, Intel Core i7, 2.50 GHz), but only one core is used for the numerical implementation.

5.1 | Example 1: A two-dimensional beam

In this example, we consider a two-dimensional beam shown in Figure 1A, which is subjected to a stochastic force $f(t,\theta)$, $t \in [0,T]$. Its finite element mesh is depicted in Figure 1B and includes $n_p = 385$ nodes and $n_e = 672$ linear triangle elements. The stochastic solution is $u(x,y,\theta) = 0$ on the boundary Γ_D. Geometric and material parameters are given by length $L = 8$ m, width $H = 1$ m, duration $T = 2$ s, mass density $2.75 \times 10^3 \mathrm{kg} \cdot \mathrm{m}^{-3}$, Poisson's ratio 0.3. The Young's modulus is modeled as a Gaussian random field with the mean value $E_0(x,y) = 60$ GPa and the modified exponential-type covariance function[49,50]

$$C_{EE}(x_1,y_1;x_2,y_2) = \sigma_E^2 \exp\left(-\frac{|x_1-x_2|}{l_x} - \frac{|y_1-y_2|}{l_y}\right)\left(1+\frac{|x_1-x_2|}{l_x}\right)\left(1+\frac{|y_1-y_2|}{l_y}\right), \tag{28}$$

where the standard deviation $\sigma_E = 0.1E_0(x,y)$ and the correlation lengths $l_x = 8$ m and $l_y = 1$ m. By use of the Karhunen–Loève (KL) expansion,[7,51,52] the random field $E(x,y,\theta)$ is approximated by the following series expansion

$$E(x,y,\theta) = E_0(x,y) + \sum_{i=1}^{r_E} \xi_i(\theta)\sqrt{\kappa_i}E_i(x,y), \tag{29}$$

where r_E is the number of truncated terms, $\{\xi_i(\theta)\}_{i=1}^{r_E}$ are independent standard Gaussian random variables and $\{\kappa_i, E_i(x,y)\}$ are the eigenvalues and eigenvectors of the covariance function solved by the following homogeneous Fredholm integral equation of the second kind

$$\int_D C_{EE}(x_1,y_1;x_2,y_2)E_i(x_1,y_1)\mathrm{d}x_1\mathrm{d}y_1 = \kappa_i E_i(x_2,y_2). \tag{30}$$

In practical implementation, to ensure that the Young's modulus is positive, the random samples $\theta^{(i)}$ such that $\min_{x,y,z\in D} E\left(x,y,z,\theta^{(i)}\right) \le 1 \times 10^{-3}$ GPa are dropped out.

Further, the force $f(t,\theta)$ is also considered as a Gaussian random process with the covariance function $C_{ff} = \sigma_f^2 \exp(|t_1-t_2|/l_t)$ and its mean function $f_0(t)$ (kN) is

$$f_0(t) = 100 - 100\exp(-3t)(1-\sin(10\pi t)). \tag{31}$$

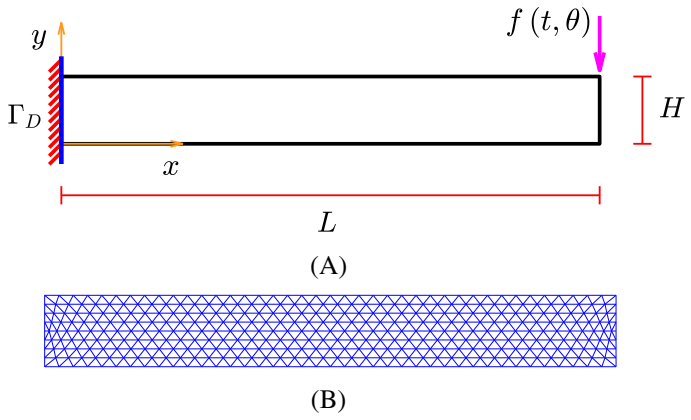

FIGURE 1 Geometric model of the beam and its finite element mesh. (A) Beam model. (B) Finite element mesh of the beam.

The stochastic force is thus approximated by KL expansion

$$f(t,\theta) = f_0(t) + \sum_{i=1}^{r_f} \eta_i(\theta)\sqrt{\chi_i} f_i(t), \tag{32}$$

where r_f is the number of the truncation and the eigenvalues and eigenvectors $\{\chi_i, f_i(t)\}$ are solved by an Equation (30)-like integral equation.

5.1.1 | Case 1: Dynamic analysis

This case considers the stochastic dynamic analysis of the given model. The time step $\Delta t = 0.01$ s is adopted for the time discretization and the number of total time steps is 201. For both this case and the static analysis in the next section, the truncated numbers r_E in (29) and r_f in Equation (32) are set as 10 and 20 stochastic dimensions are thus involved in total. The iterative errors $\epsilon_{\text{ev},j}$ in Algorithm 3 corresponding to different retained terms $\{\mathbf{d}_j\}$ are shown in Figure 2. Only 6 terms are retained to achieve the specified precision, which indicates the good convergence rate of the proposed method. It is noted that since the stochastic eigenvalues $\{\lambda_j(\theta)\}_{j=1}^{6}$ are recomputed by Equation (19) and those used to calculate the iterative error $\epsilon_{\text{ev},j}$ are not the final solutions, $\epsilon_{\text{ev},j}$ is only considered as an indicator error. In our experience, it is a good checker for a high-accuracy approximation of the stochastic solution. Deterministic vectors $\{\mathbf{d}_{j,y}\}_{j=1}^{6}$ in the y direction are seen from Figure 3. Similar to the deterministic case, more high-order modes are captured as the number of retained terms increases, which provides high-accuracy deterministic bases to approximate the stochastic solution. To verify the computational accuracy of Algorithm 3, we compare the probability density functions (PDFs) of the stochastic eigenvalues solved by Equation (19) and MCS in Figure 4, which demonstrates that all stochastic eigenvalues obtained by Algorithm 3 are well matched with that by MCS.

Based on the stochastic eigenvalues and the stochastic eigenvectors obtained by Algorithm 3, we solve the original stochastic dynamic equation using Algorithm 1. To test the computational accuracy of the proposed method, PDFs of the stochastic displacements of the point $(x, y) = (8, 0.5)$ at the time $t = 1$ s in the y direction obtained by the proposed SMD and MCS are compared in Figure 5, which shows that the proposed SMD has a good agreement with MCS. In Figure 5, we also provide the PDF obtained by the reduced-order method (ROM) given in Remark 1, which also achieves a good agreement with MCS. Hence, combining Algorithm 3 and the ROM in Remark 1 is also suggested to be a good choice to solve stochastic dynamic problems. To show the computational efficiency, computational times of all three methods are listed in Table 1. The times for calculating the deterministic matrix $\mathbf{D} \in \mathbb{R}^{770\times 6}$, the stochastic matrix $\mathbf{\Pi}(\theta) \in \mathbb{R}^{6\times 6}$ and the time-dependent stochastic vector $\mathbf{q}(t,\theta) \in \mathbb{R}^{6\times 201}$ represent the computational costs of step 2 to step 11 of Algorithm 3,

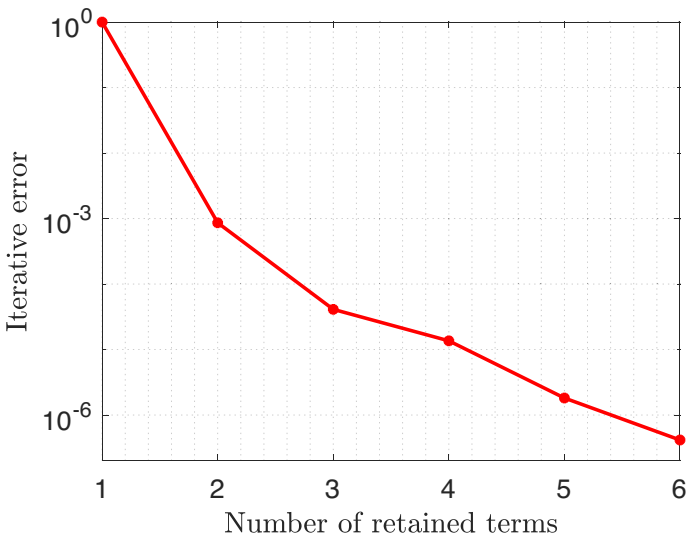

FIGURE 2 Iterative errors of different numbers of retained terms.

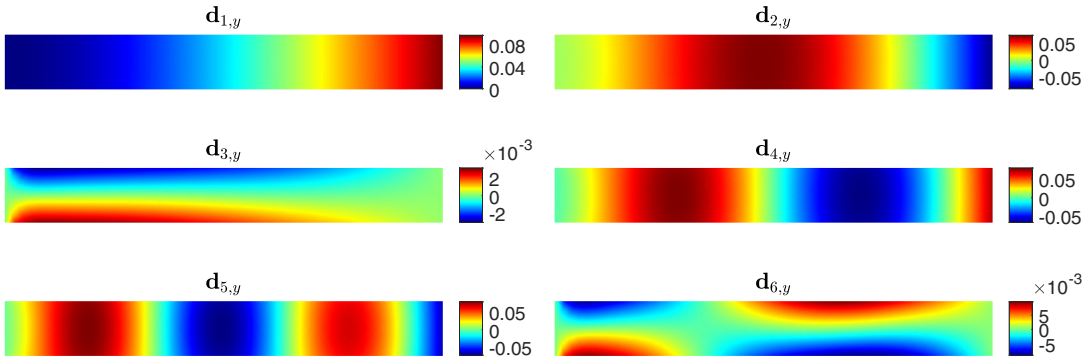

FIGURE 3 Deterministic vectors $\{\mathbf{d}_{j,y}\}_{j=1}^{6}$ in the y direction.

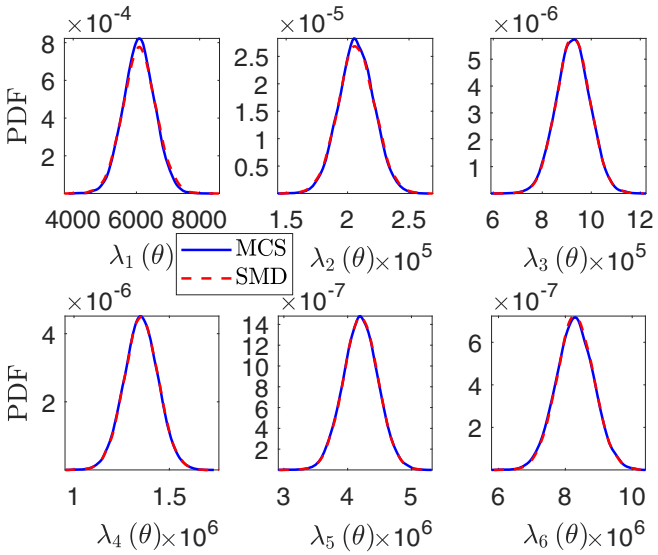

FIGURE 4 PDFs of the stochastic eigenvalues $\{\lambda_i(\theta)\}_{i=1}^{6}$.

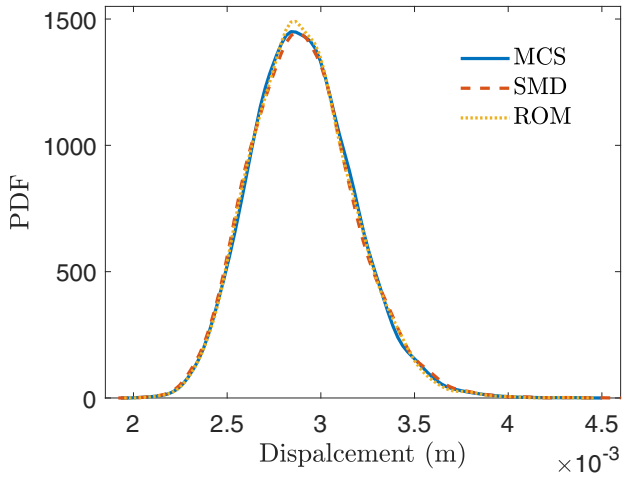

FIGURE 5 PDFs of the stochastic displacements $u(x, y, t, \theta)$ of the point $(x, y) = (8, 0.5)$ at the time $t = 1$ s in the y direction obtained by MCS, the proposed SMD and the ROM given in Remark 1, respectively.

TABLE 1 Computational times for solving the components in Equations (25) and (26).

Time for	D	$\mathbf{\Pi}(\theta)$	$\mathbf{q}(t,\theta)$	Total time (s)
SMD	1.47	1.24	5.73	8.44
ROM	1.47	–	7.12	8.59
MCS	–	–	–	1.03×10^4

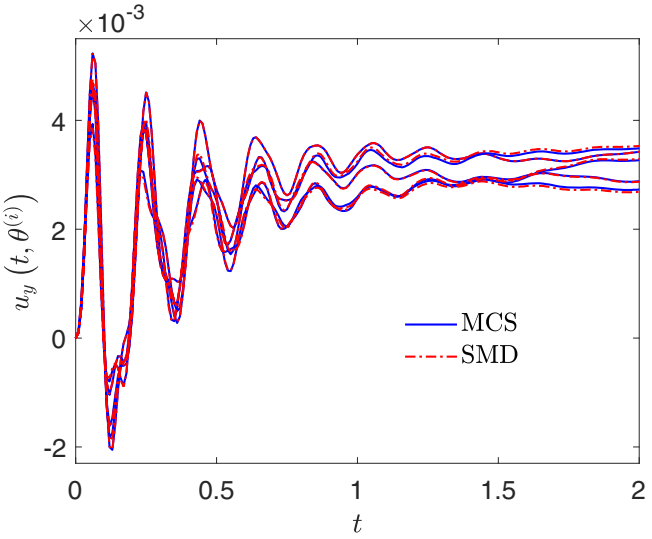

FIGURE 6 Five sample realizations of the stochastic displacements $u(x,y,t,\theta)$ of the point $(x,y) = (8, 0.5)$ in the y direction obtained by MCS and the proposed SMD, respectively.

step 12 of Algorithm 3 and step 2 to step 10 of Algorithm 1, respectively. It is seen that both SMD and ROM are much more efficient than MCS and a thousandfold speedup is achieved. The ROM does not involve the calculation of the stochastic matrix $\mathbf{\Pi}(\theta)$ since the deterministic matrix $\mathbf{D}$ is used to construct the reduced-order dynamic equation directly. SMD is a bit faster than ROM in solving the time-dependent stochastic vector $\mathbf{q}(t,\theta)$ since only SDoF stochastic dynamic equations are solved in SMD, while small systems of linear stochastic dynamic equations require to be solved in ROM. As the number of retained terms $\{\mathbf{d}_i\}$ and/or the number of total time steps increase, the computational effort for solving $\mathbf{q}(t,\theta)$ by ROM is slightly higher than that of SMD.

We highlight that the proposed method has very high accuracy even for each sample realization $\theta^{(i)}$. To show this point, five sample realizations of the stochastic displacements $u(x,y,t,\theta)$ of the point $(x,y) = (8, 0.5)$ in the y direction obtained by the proposed SMD and MCS are compared in Figure 6. For each sample realization and each time step, the solution obtained by SMD well matches that by MCS. In this sense, the proposed SMD also provides a high-accuracy reduced-order model for the original stochastic dynamic equation. As discussed in Remark 1, the ROM can also achieve this purpose. We do not provide further numerical illustrations for this point here.

Further, it is seen from Figure 6 that the stochastic displacements decay quickly. To demonstrate the promising performance of the proposed method, we consider a slowly decaying stochastic excitation by changing the mean function $f_0(t)$ of the stochastic force $f(t,\theta)$ in Equation (32) to $f_0^*(t)$

$$f_0^*(t) = 100 - 100\exp(-t)(1 - \sin(30\pi t)), \tag{33}$$

which decays much more slowly than $f_0(t)$, as compared in Figure 7. It is noted that only the stochastic excitation is changed here, so the above stochastic eigenvectors can be reused. In this way, only the right-side term $h_i(t,\theta)$ in Equation (9) is recalculated, which is computationally cheap. Five sample realizations of the stochastic displacements $u(x,y,t,\theta)$ of the point $(x,y) = (8, 0.5)$ in the y direction under the slowly decaying stochastic excitation obtained by MCS and the proposed SMD are shown in Figure 8, which indicates that the proposed method is still very accurate for each sample realization $\theta^{(i)}$.

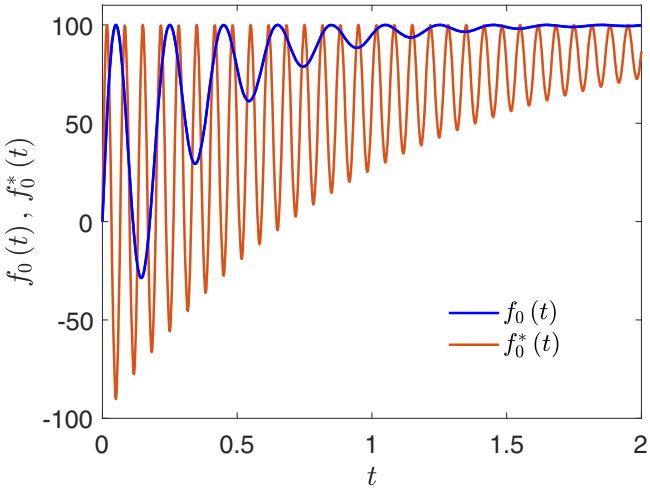

FIGURE 7 Comparison of the mean functions $f_0(t)$ in Equation (31) and $f_0^*(t)$ in Equation (33).

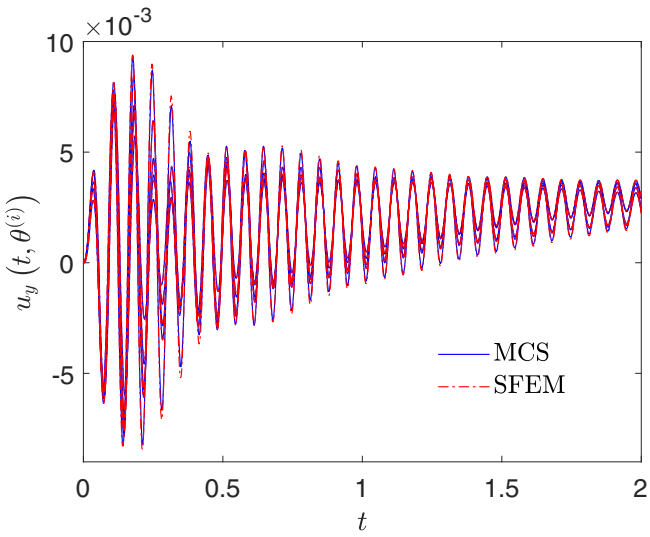

FIGURE 8 Five sample realizations of the stochastic displacements $u(x, y, t, \theta)$ of the point $(x, y) = (8, 0.5)$ in the y direction under the slowly decaying stochastic excitation obtained by MCS and the proposed SMD, respectively.

5.1.2 | Case 2: Static analysis

In this case, we consider the stochastic static analysis of the problem and a stochastic vertical force given by $f(t = T, \theta)$ is applied to the same position. To generate the stochastic subspace, a standard stochastic eigenvalue equation is solved using Algorithm 3 and 6 terms $\{\mathbf{d}_j\}_{j=1}^{6}$ are retained to meet the specified precision. As shown in Figure 9, the PDFs of the stochastic displacements $u(x, y, \theta)$ of the point $(x, y) = (8, 0.5)$ in the y direction obtained by both the proposed SMD and ROM have comparable accuracy with that obtained by MCS, which indicates that the proposed two methods still work well for stochastic static problems. Computational times of the three methods for this case are listed in Table 2, which shows that both SMD and ROM are still much more efficient than MCS. SMD is very cheap due to only the element-wise division operation of sample vectors involved, which weakly depends on the sample size. While the computational cost for solving the reduced-order stochastic finite element equation arising in ROM linearly depends on the sample size. The total cost of ROM is a bit cheaper than that of SMD since there is no cost spent on the solution of the stochastic matrix $\mathbf{\Pi}(\theta)$.

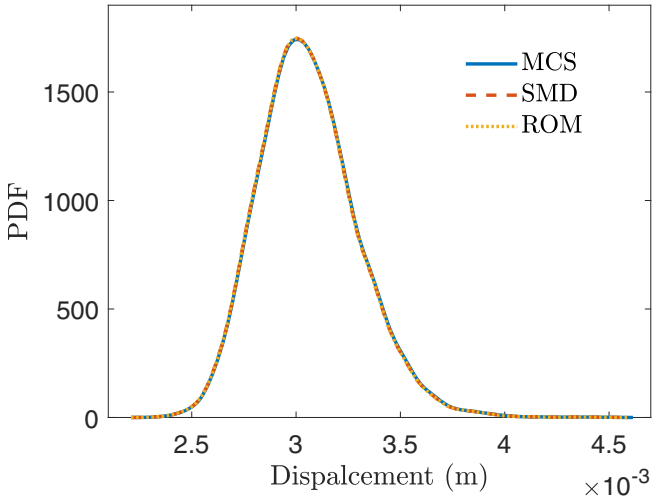

FIGURE 9 PDFs of the stochastic displacements $u(x, y, \theta)$ of the point $(x, y) = (8, 0.5)$ in the y direction obtained by MCS, the proposed SMD and the ROM given in Remark 1, respectively.

TABLE 2 Computational times for solving the components in Equations (24) and (27).

Time for	D	$\mathbf{\Pi}(\theta)$	$\mathbf{q}(\theta)$	Total time (s)
SMD	1.44	1.28	0.12	2.84
ROM	1.44	–	0.68	2.12
MCS	–	–	–	467.36

TABLE 3 Computational times for solving the components in Equations (25) and (26) when the stochastic dimension is 100.

Time for	D	$\mathbf{\Pi}(\theta)$	$\mathbf{q}(t, \theta)$	Total time (s)	MCS
$r = 20$	1.47	1.24	5.73	8.44	1.03×10^4
$r = 100$	1.81	1.39	7.66	10.86	1.14×10^4

5.1.3 | Case 3: High-dimensional dynamic analysis

In this case, we perform the dynamic analysis with high stochastic dimensions. The truncated numbers r_E in Equation (29) and r_f in Equation (32) are set as 50 and 100 stochastic dimensions are involved in total. Other parameters of the problem are the same as that given in Section 5.1.1. 10 vectors $\{\mathbf{d}_j\}_{j=1}^{10}$ are retained by a generalized high-dimensional stochastic eigenproblem. Computational times of the proposed SMD and MCS for this case are shown in Table 3. As a comparison, corresponding computational costs for the low-dimensional case studied in Section 5.1.1 are also listed in Table 3. It is seen that SMD is still much cheaper than MCS for high-dimensional stochastic cases. Compared to the low-dimensional case, the computational times for solving all three components $\mathbf{D}$, $\mathbf{\Pi}(\theta)$ and $\mathbf{q}(t, \theta)$ has only increased a little bit, which indicates that the proposed SMD is weakly dependent on the stochastic dimension. In this way, the curse of dimensionality arising in high-dimensional stochastic problems is avoided successfully. Further, to show the computational accuracy of high-dimensional stochastic cases, PDFs of the stochastic displacements $u(x, y, t, \theta)$ of the point $(x, y) = (8, 0.5)$ at the time $t = 1$ s in the y direction obtained by MCS and SMD are compared in Figure 10, which demonstrates that the proposed SMD still has high accuracy for high-dimensional stochastic cases. It is noted that the PDFs in Figure 10 are close to that in Figure 5 since some last truncated terms in Equations (29) and (32) have little contributions to the randomness. We can adopt some truncation criteria to choose the truncated numbers. In this article, we just use high-dimensional truncation to test the proposed method. In the practical implementation, the proposed SMD performs the same calculation for both low- and high-dimensional cases. If the high-dimensional truncation contributes a lot to the random fields, only more vectors $\mathbf{d}_j$ are retained to approximate the final stochastic solution.

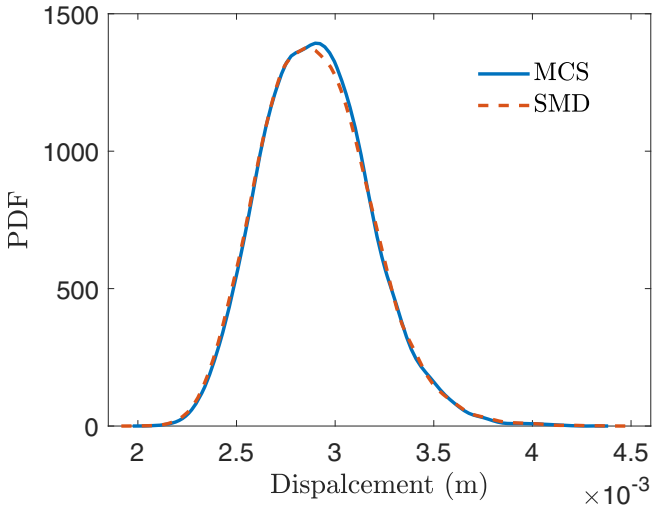

FIGURE 10 PDFs of the stochastic displacements $u(x, y, t, \theta)$ of the point $(x, y) = (8, 0.5)$ at the time $t = 1$ s in the y direction obtained by MCS and the proposed SMD when the stochastic dimension is 100.

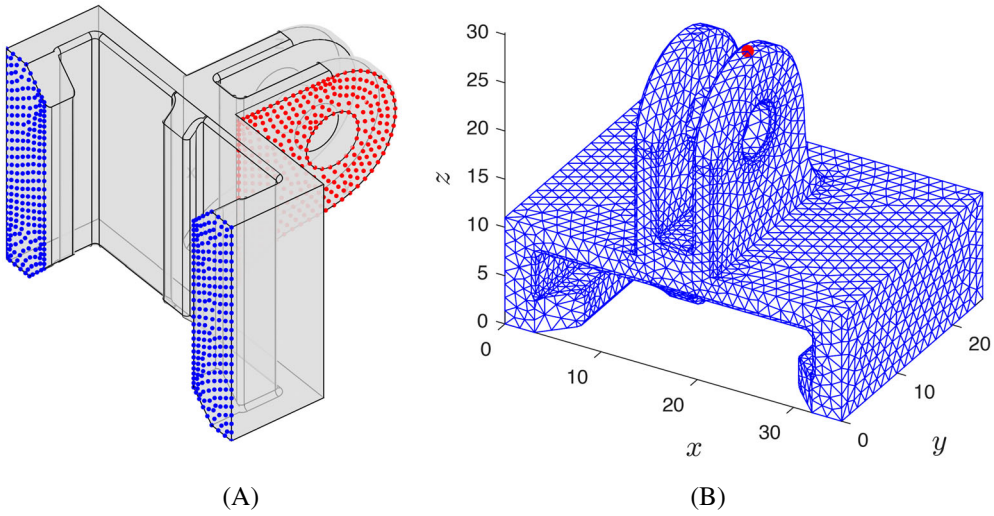

FIGURE 11 Geometric model of the mechanical part and its finite element mesh. (A) Model of the mechanical part. (B) Finite element mesh of the mechanical part.

5.2 | Example 2: A three-dimensional mechanical part

This example considers a three-dimensional mechanical part shown in Figure 11A, where the Dirichlet boundary condition $u(x, y, z, \theta) = 0$ holds on the blue surface. An external force P is applied to the red surface along the x direction (see Figure 11B) and its value is 500 kN/m^2 for $t \in [0, t_0]$ and 0 for $t \in (t_0, 1]$, where the duration $t_0 = 0.1$ s. The finite element mesh is depicted in Figure 11B (unit: cm) and it includes $n_p = 6685$ nodes, $n_e = 26{,}819$ linear tetrahedral elements and 20,055 degrees of freedom in total.

The Young's modulus is modeled as a Gaussian random field with the mean value $E_0(x, y) = 209$ GPa and the covariance function

$$C_{EE}(x_1, y_1, z_1; x_2, y_2, z_2) = \sigma_E^2 \exp\left(-\frac{|x_1 - x_2|}{l_x} - \frac{|y_1 - y_2|}{l_y} - \frac{|z_1 - z_2|}{l_z}\right), \tag{34}$$

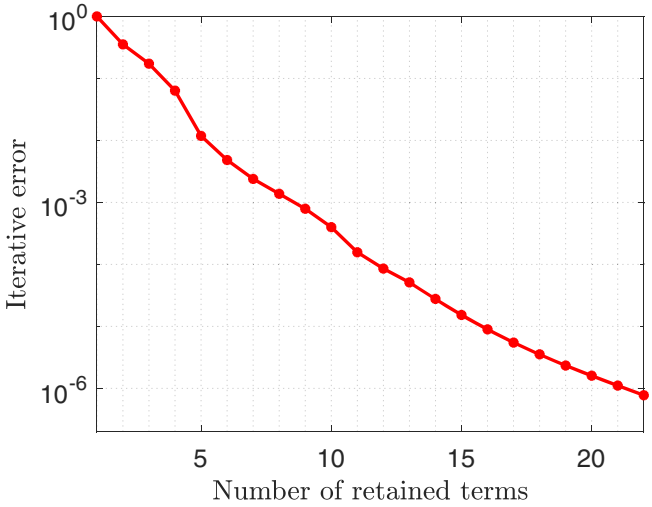

FIGURE 12 Iterative errors of different numbers of retained terms.

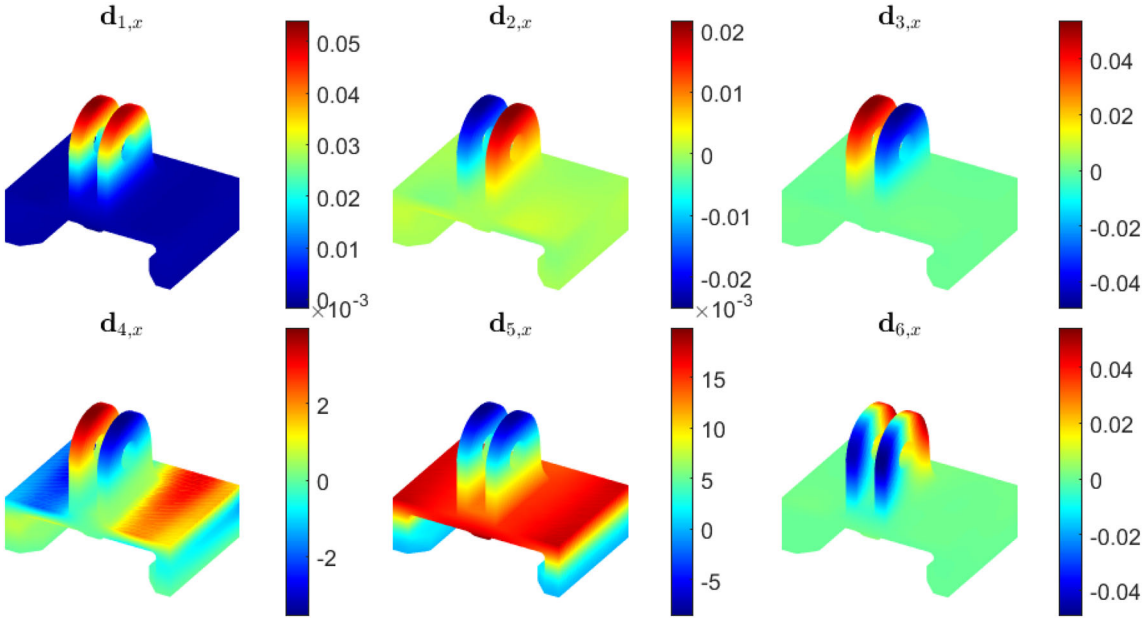

FIGURE 13 The first six deterministic vectors $\{\mathbf{d}_{i,x}\}_{i=1}^{6}$ in the x direction.

where the standard derivation $\sigma_E = 0.1E_0(x, y)$, the correlation lengths are $l_{x_i} = \max x_i - \min x_i, x_i = x, y, z$. In the numerical investigation, we adopt Equation (29)-like 10-term truncated KL expansion to approximate the Young's modulus and the random samples $\theta^{(i)}$ such that $\min_{x,y,z\in D} E(x, y, z, \theta^{(i)}) \leq 1 \times 10^{-3}$ GPa are dropped out to ensure that all realizations are positive. Other material properties are given by mass density 7.80×10^3 kg $\cdot$ m^{-3} and Poisson's ratio 0.3.

5.2.1 | Case 1: Dynamic analysis

In this case, the time step $\Delta t = 0.01$ s is adopted for the time discretization and 100 time steps are thus obtained. The iterative errors $\epsilon_{\text{ev},j}$ of different retained terms $\{\mathbf{d}_j\}_j$ are shown in Figure 12 and it requires 22 terms to meet the specified precision. Compared to the case in Example 5.1.1, more terms are retained due to a more complex geometry involved. The corresponding first six deterministic vectors $\{\mathbf{d}_{j,x}\}_{j=1}^{6}$ in the x direction are depicted in Figure 13. It is seen that several local modes of the upper part are well captured.

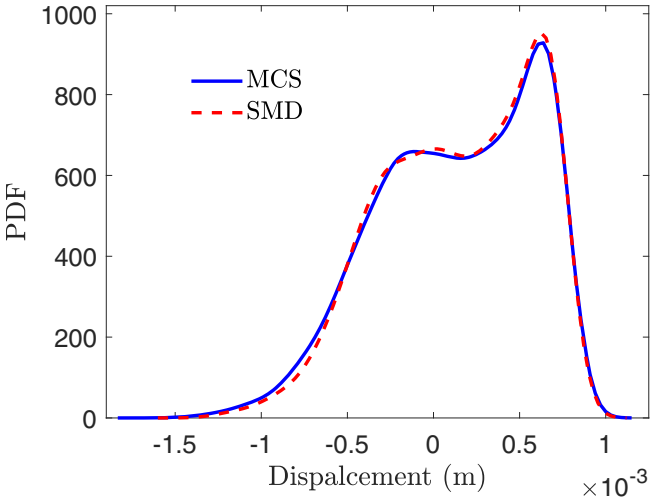

FIGURE 14 PDFs of the stochastic displacements $u(x, y, z, t, \theta)$ of the red point (shown in Figure 11B) at the time $t = 0.5$ s in the x direction obtained by MCS, the proposed SMD, respectively.

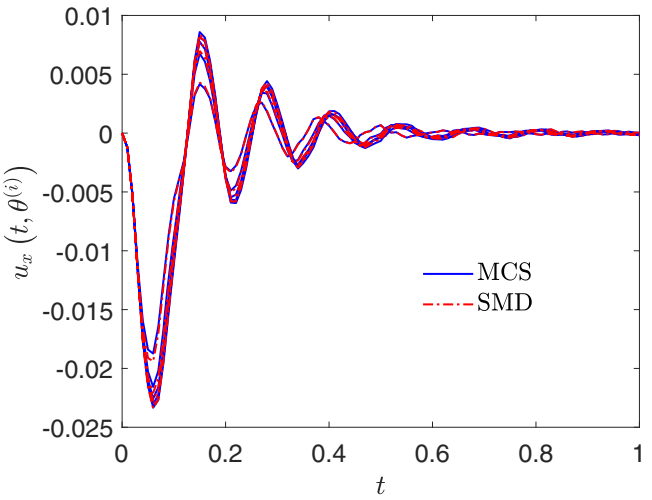

FIGURE 15 Five sample realizations obtained by MCS and the proposed SMD, respectively.

PDFs of the stochastic displacements of the red point (shown in Figure 11B) at the time $t = 0.5$ s in the x direction obtained by the proposed SMD and MCS are compared in Figure 14, which again verifies the high accuracy of the proposed method. Since the external force disappears at the time $t = 0.1$ s, for the time $t > 0.1$ s, the problem can be considered as a free stochastic vibration with the stochastic initial displacement and velocity given at the time $t = 0.1$ s. The stochastic displacement at the time $t = 0.5$ s induced by the free vibration is related to the stochastic initial values and the stochastic stiffness matrix, and their values may be positive or negative. Also, five sample realizations of the stochastic displacement $u(x, y, z, t, \theta)$ of the red point in the x direction obtained by the proposed SMD and MCS are compared in Figure 15. For each sample realization, the results obtained by the two methods are in good accordance, thus using the proposed SMD as a stochastic reduced-order method is still accurate enough. Computational times for this case are listed in the first line of Table 4, which indicates that the total computational time of the proposed method is much less than that of MCS. Most computational effort is used for the deterministic matrix $\mathbf{D} \in \mathbb{R}^{20055\times22}$ since solving large-scale deterministic eigenvalue equations is time-consuming. The computational time for solving the stochastic matrix $\mathbf{\Pi}(\theta) \in \mathbb{R}^{22\times22}$ only depends on the number of retained terms, thus it is cheap to be solved in both this example and the Example 5.1. The computational cost for the time-dependent stochastic vector $\mathbf{q}(t, \theta) \in \mathbb{R}^{22\times101}$ is a bit more expensive in this case due to a larger number of the retained terms, but it is still cheap enough compared to the total computational time.

TABLE 4 Computational times for solving the components in Equations (25) and (26).

Time for	D	$\Pi(\theta)$	$\mathbf{q}(t,\theta)$	Total time (s)	MCS
Dynamic case	489.29	3.14	13.25	505.68	3.89×10^4
Static case	417.81	2.90	0.21	420.92	7.02×10^3

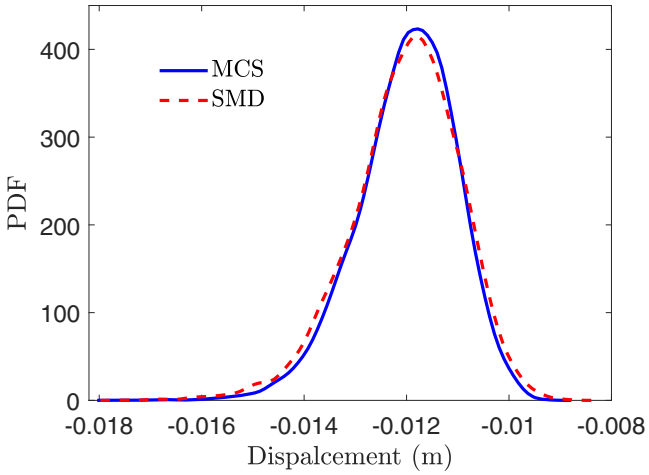

FIGURE 16 PDFs of the stochastic displacements $u(x, y, z, \theta)$ of the red point (shown in Figure 11B) in the x direction obtained by MCS and the proposed SMD, respectively.

5.2.2 | Case 2: Static analysis

The stochastic static analysis of the problem is performed in this case. The external force P is applied to the model in the same way but its value is fixed as 500 kN/m^2. 20 terms $\{\mathbf{d}_j\}_{j=1}^{20}$ are obtained by solving the standard stochastic eigenvalue equation. PDFs of the stochastic displacement $u(x, y, z, \theta)$ of the red point (shown in Figure 11B) in the x direction obtained by the proposed SMD and MCS are depicted in Figure 16, which indicates that the proposed method still provides comparable accuracy to MCS. If a higher-accuracy stochastic solution is required in some cases, it can be achieved by increasing the number of retained terms $\{\mathbf{d}_j\}_j$. Computational times for this case are listed in the second line of Table 4. Similar to the stochastic dynamic case, the most computational cost is used for the deterministic matrix $\mathbf{D} \in \mathbb{R}^{20055\times 20}$. In this case, the computational cost for each component in Table 4 is less than that for the dynamic case, especially for solving the time-independent stochastic vector $\mathbf{q}(\theta) \in \mathbb{R}^{20}$, since only 20 time-independent stochastic algebraic equations need to be solved.

6 | CONCLUSIONS

In this article, we presented novel stochastic modal decomposition-based numerical schemes for solving both stochastic static and dynamic problems. By an efficient reduced-order method, standard/generalized stochastic eigenvalue equations are first solved to calculate stochastic eigenvectors and generate stochastic subspaces. The stochastic solutions of both stochastic static and dynamic problems are then represented as stochastic linear combinations of bases of the stochastic subspaces. Original stochastic static/dynamic equations are thus transformed into a set of SDoF stochastic static/dynamic equations. The SDoF stochastic dynamic equations can be efficiently solved by a non-intrusive stochastic Newmark approach and the SDoF stochastic static equations are solved by an element-wise division operation of random sample vectors. The proposed methods can be applied to high-dimensional stochastic problems without any modification and much extra computational effort, which has been verified via a numerical example of up to a hundred stochastic dimensions. In these senses, the proposed methods provide effective ways and novel perspectives for structural static and dynamic analysis involving uncertainties.

ACKNOWLEDGMENTS

The authors are grateful to the Alexander von Humboldt Foundation, the German Research Foundation (DFG) project (Grant number 527222589) and the International Research Training Group 2657 (IRTG 2657) funded by the DFG (Grant number 433082294). Open Access funding enabled and organized by Projekt DEAL.

DATA AVAILABILITY STATEMENT

Data sharing is not applicable to this article as no new data were created or analyzed in this study.

ORCID

Zhibao Zheng https://orcid.org/0000-0003-4189-8817

REFERENCES

1. Papadrakakis M, Papadopoulos V. Robust and efficient methods for stochastic finite element analysis using Monte Carlo simulation. *Comput Methods Appl Mech Eng*. 1996;134(3-4):325-340.
2. Caflisch RE. Monte Carlo and quasi-Monte Carlo methods. *Acta Numer*. 1998;7:1-49.
3. Giles MB. Multilevel Monte Carlo methods. *Acta Numer*. 2015;24:259-328.
4. Fuhg JN, Fau A, Nackenhorst U. State-of-the-art and comparative review of adaptive sampling methods for kriging. *Arch Comput Methods Eng*. 2021;28:1-59.
5. Khuri AI, Mukhopadhyay S. Response surface methodology. *Wiley Interdiscip Rev Comput Stat*. 2010;2(2):128-149.
6. Doostan A, Validi A, Iaccarino G. Non-intrusive low-rank separated approximation of high-dimensional stochastic models. *Comput Methods Appl Mech Eng*. 2013;263:42-55.
7. Ghanem RG, Spanos PD. *Stochastic finite Elements: A Spectral Approach*. Courier Corporation; 2003.
8. Xiu D, Karniadakis GE. The Wiener-Askey polynomial chaos for stochastic dierential equations. *SIAM J Sci Comput*. 2002;24(2):619-644.
9. Matthies HG, Keese A. Galerkin methods for linear and nonlinear elliptic stochastic partial differential equations. *Comput Methods Appl Mech Eng*. 2005;194(12-16):1295-1331.
10. Pellissetti MF, Ghanem RG. Iterative solution of systems of linear equations arising in the context of stochastic finite elements. *Adv Eng Softw*. 2000;31(8-9):607-616.
11. Blatman G, Sudret B. An adaptive algorithm to build up sparse polynomial chaos expansions for stochastic finite element analysis. *Prob Eng Mech*. 2010;25(2):183-197.
12. Eldred M. Recent advances in non-intrusive polynomial chaos and stochastic collocation methods for uncertainty analysis and design. *50th AIAA/ASME/ASCE/AHS/ASC Structures, Structural Dynamics, and Materials Conference*. AIAA; 2009:2274.
13. Lee GY, Park YH. A proper generalized decomposition-based harmonic balance method with arc-length continuation for nonlinear frequency response analysis. *Comput Struct*. 2023;275:106913.
14. Chevreuil M, Nouy A. Model order reduction based on proper generalized decomposition for the propagation of uncertainties in structural dynamics. *Int J Numer Methods Eng*. 2012;89(2):241-268.
15. Gao L, Audouze C, Nair PB. Anchored analysis of variance Petrov–Galerkin projection schemes for linear stochastic structural dynamics. *Proc Royal Soc A Math Phys Eng Sci*. 2015;471(2182):20150023.
16. Chen G, Yang D. Direct probability integral method for stochastic response analysis of static and dynamic structural systems. *Comput Methods Appl Mech Eng*. 2019;357:112612.
17. Huo H, Xu W, Wang W, Chen G, Yang D. New non-intrusive stochastic finite element method for plate structures. *Comput Struct*. 2022;268:106812.
18. Bathe KJ. *Finite Element Procedures*. Klaus-Jurgen Bathe; 2006.
19. Hughes TJ. *The Finite Element Method: Linear Static and Dynamic Finite Element Analysis*. Courier Corporation; 2012.
20. Pradlwarter H, Schuëller G, Szekely G. Random eigenvalue problems for large systems. *Comput Struct*. 2002;80(27-30):2415-2424.
21. Gilbert AD, Scheichl R. Multilevel quasi-Monte Carlo for random elliptic eigenvalue problems II: Efficient algorithms and numerical results. arXiv preprint, arXiv:2103.03407; 2021.
22. Adhikari S, Friswell M. Random matrix eigenvalue problems in structural dynamics. *Int J Numer Methods Eng*. 2007;69(3):562-591.
23. Pascual B, Adhikari S. Hybrid perturbation-polynomial chaos approaches to the random algebraic eigenvalue problem. *Comput Methods Appl Mech Eng*. 2012;217:153-167.
24. Hao P, Tang H, Wang Y, Wu T, Feng S, Wang B. Stochastic isogeometric buckling analysis of composite shell considering multiple uncertainties. *Reliab Eng Syst Saf*. 2023;230:108912.
25. Ghanem R, Ghosh D. Efficient characterization of the random eigenvalue problem in a polynomial chaos decomposition. *Int J Numer Methods Eng*. 2007;72(4):486-504.
26. Pagnacco E, Cursi dES, Sampaio R. Subspace inverse power method and polynomial chaos representation for the modal frequency responses of random mechanical systems. *Comput Mech*. 2016;58(1):129-149.
27. Lee K, Sousedik B. Inexact methods for symmetric stochastic eigenvalue problems. *SIAM/ASA J Uncertain Quantificat*. 2018;6(4):1744-1776.
28. Ghosh D, Ghanem R. An invariant subspace-based approach to the random eigenvalue problem of systems with clustered spectrum. *Int J Numer Methods Eng*. 2012;91(4):378-396.

29. Adhikari S, Chakraborty S. Random matrix eigenvalue problems in structural dynamics: An iterative approach. *Mech Syst Signal Process*. 2022;164:108260.
30. Lan J, Dong X, Peng Z, Zhang W, Meng G. Uncertain eigenvalue analysis by the sparse grid stochastic collocation method. *Acta Mech Sinica*. 2015;31(4):545-557.
31. Rahman S. A solution of the random eigenvalue problem by a dimensional decomposition method. *Int J Numer Methods Eng*. 2006;67(9):1318-1340.
32. Rahman S, Jahanbin R. A spline dimensional decomposition for uncertainty quantification in high dimensions. *SIAM/ASA J Uncertain Quantif*. 2022;10(1):404-438.
33. Huang B, Zhang H, Phoon KK. Homotopy approach for random eigenvalue problem. *Int J Numer Methods Eng*. 2018;113(3):450-478.
34. Benner P, Onwunta A, Stoll M. A low-rank inexact Newton–Krylov method for stochastic eigenvalue problems. *Comput Methods Appl Math*. 2019;19(1):5-22.
35. Elman HC, Su T. Low-rank solution methods for stochastic eigenvalue problems. *SIAM J Sci Comput*. 2019;41(4):A2657-A2680.
36. Sepahvand K, Marburg S, Hardtke HJ. Stochastic structural modal analysis involving uncertain parameters using generalized polynomial chaos expansion. *Int J Appl Mech*. 2011;3(3):587-606.
37. Ghosh D. Application of the random eigenvalue problem in forced response analysis of a linear stochastic structure. *Arch Appl Mech*. 2013;83(9):1341-1357.
38. Sarkar S, Ghosh D. A hybrid method for stochastic response analysis of a vibrating structure. *Arch Appl Mech*. 2015;85(11):1607-1626.
39. Yang J, Faverjon B, Peters H, Marburg S, Kessissoglou N. Deterministic and stochastic model order reduction for vibration analyses of structures with uncertainties. *J Vib Acoust*. 2017;139(2):021007.
40. Kasinos S, Palmeri A, Lombardo M, Adhikari S. A reduced modal subspace approach for damped stochastic dynamic systems. *Comput Struct*. 2021;257:106651.
41. Rahman S, Jahanbin R. Orthogonal spline expansions for uncertainty quantification in linear dynamical systems. *J Sound Vib*. 2021;512:116366.
42. Zheng Z, Beer M, Nackenhorst U. An efficient reduced-order method for stochastic eigenvalue analysis. *Int J Numer Methods Eng*. 2022;123:1-23.
43. Bathe KJ, Ramaswamy S. An accelerated subspace iteration method. *Comput Methods Appl Mech Eng*. 1980;23(3):313-331.
44. Butcher JC. *Numerical Methods for Ordinary Differential Equations*. John Wiley & Sons; 2016.
45. Saad Y. *Numerical Methods for Large Eigenvalue Problems*. SIAM; 2011.
46. Paz M. *Structural Dynamics: Theory and Computation*. Springer Science & Business Media; 2012.
47. Zheng Z, Beer M, Dai H, Nackenhorst U. A weak-intrusive stochastic finite element method for stochastic structural dynamics analysis. *Comput Methods Appl Mech Eng*. 2022;399:115360.
48. Zheng Z, Dai H. Structural stochastic responses determination via a sample-based stochastic finite element method. *Comput Methods Appl Mech Eng*. 2021;381:113824.
49. Spanos PD, Beer M, Red-Horse J. Karhunen–Loève expansion of stochastic processes with a modified exponential covariance kernel. *J Eng Mech*. 2007;133(7):773-779.
50. Faes MG, Broggi M, Spanos PD, Beer M. Elucidating appealing features of differentiable auto-correlation functions: A study on the modified exponential kernel. *Prob Eng Mech*. 2022;69:103269.
51. Zheng Z, Dai H. Simulation of multi-dimensional random fields by Karhunen–Loève expansion. *Comput Methods Appl Mech Eng*. 2017;324:221-247.
52. Zheng Z, Dai H, Wang Y, Wang W. A sample-based iterative scheme for simulating non-stationary non-Gaussian stochastic processes. *Mech Syst Signal Process*. 2021;151:107420.

How to cite this article: Zheng Z, Beer M, Nackenhorst U. Efficient stochastic modal decomposition methods for structural stochastic static and dynamic analyses. *Int J Numer Methods Eng*. 2024;e7469. doi: 10.1002/nme.7469

APPENDIX

Proof of Equation (5)

Proof. Multiplying the stochastic eigenequation (4) corresponding to the stochastic mode $\boldsymbol{\varphi}_j(\theta)$ (and $\boldsymbol{\varphi}_i(\theta)$) by $\boldsymbol{\varphi}_i^{\mathrm{T}}(\theta)$ (and $\boldsymbol{\varphi}_j^{\mathrm{T}}(\theta)$) from left we have

$$\boldsymbol{\varphi}_i^{\mathrm{T}}(\theta)\mathbf{K}(\theta)\boldsymbol{\varphi}_j(\theta) = \lambda_j(\theta)\boldsymbol{\varphi}_i^{\mathrm{T}}(\theta)\mathbf{M}(\theta)\boldsymbol{\varphi}_j(\theta), \tag{A1}$$

$$\boldsymbol{\varphi}_j^{\mathrm{T}}(\theta)\mathbf{K}(\theta)\boldsymbol{\varphi}_i(\theta) = \lambda_i(\theta)\boldsymbol{\varphi}_j^{\mathrm{T}}(\theta)\mathbf{M}(\theta)\boldsymbol{\varphi}_i(\theta). \tag{A2}$$

Due to $\boldsymbol{\varphi}_i^{\mathrm{T}}(\theta)\mathbf{K}(\theta)\boldsymbol{\varphi}_j(\theta) \equiv \boldsymbol{\varphi}_j^{\mathrm{T}}(\theta)\mathbf{K}(\theta)\boldsymbol{\varphi}_i(\theta)$ and $\boldsymbol{\varphi}_i^{\mathrm{T}}(\theta)\mathbf{M}(\theta)\boldsymbol{\varphi}_j(\theta) \equiv \boldsymbol{\varphi}_j^{\mathrm{T}}(\theta)\mathbf{M}(\theta)\boldsymbol{\varphi}_i(\theta)$, subtracting Equation (A2) from Equation (A1) we have

$$\big(\lambda_j(\theta) - \lambda_i(\theta)\big)\boldsymbol{\varphi}_i^{\mathrm{T}}(\theta)\mathbf{M}(\theta)\boldsymbol{\varphi}_j(\theta) = 0 \qquad \text{a.e.}, \tag{A3}$$

thus $\boldsymbol{\varphi}_i^{\mathrm{T}}(\theta)\mathbf{M}(\theta)\boldsymbol{\varphi}_j(\theta) = 0$ holds due to the stochastic eigenvalues $\lambda_j(\theta) \neq \lambda_i(\theta)$. Further, substituting $\boldsymbol{\varphi}_i^{\mathrm{T}}(\theta)\mathbf{M}(\theta)\boldsymbol{\varphi}_j(\theta) = 0$ into Equation (A1) we have $\boldsymbol{\varphi}_i^{\mathrm{T}}(\theta)\mathbf{K}(\theta)\boldsymbol{\varphi}_j(\theta) = 0$. ■